Data Repository DR2009068

Supplemental Data File

Feinberg et al., 2009

Age Constraints on Alleged 'Footprints' Preserved in the Xalnene Tuff near Puebla, Mexico

The accompanying pages include additional evidence for Cerro Toluquilla as the source volcano for the Xalnene Tuff, supporting rock magnetic data for tuff and lava samples, a detailed data table for the paleomagnetic results, and a description of the methodology used in our $^{40}Ar/^{39}Ar$ analyses.

Figure DR1. Apparent $^{40}Ar/^{39}Ar$ age and Ca/K spectra for subsamples of basalt from Cerro Toluquilla volcano.

Figure DR2. Isothermal remanent magnetization data for typical lapillus

Figure DR3. Strong-field thermomagnetic curves for typical lapillus.

Figure DR4. First-order reversal curve diagram for typical lapillus.

Figure DR5. Mass-normalized susceptibility curve for Cerro Toluquillo Lava.

Table DR1. $^{40}Ar/^{39}$ Results in tabular form

Table DR2. Paleomagnetic Results Data Table

Text: $^{40}Ar/^{39}Ar$ Methodology

Supplementary Information for $^{40}Ar/^{39}Ar$ methods

$^{40}Ar/^{39}Ar$ methods. Samples were crushed, ground, sieved to the 250-420 micron size fraction, and rinsed ultrasonically in ~3% HF for 5 minutes. Olivine phenocrysts were removed by hand-picking, and ~200 mg of groundmass was irradiated for 0.5 hr in the CLICIT facility of OSTR reactor along with the 1.193 Ma Alder Creek sanidine (ACs) standard (Nomade et al., 2005). Approximately 75 mg of sample was degassed incrementally in nine steps in each of two experiments. Degassing in each experiment used a CO_2 laser whose 2-30 W beam was dispersed by an integrator lens. Ar isotope ions beams were measured with a Balzers electron multiplier in analog mode, using 10 cycles of peak-hopping to measure ^{40}Ar, ^{39}Ar, ^{38}Ar, ^{37}Ar, and ^{36}Ar. Blanks were measured between every 3 steps, and the blank correction comprised an average value over the course of the run. Mass discrimination was monitored through analysis of air aliquots delivered by an automated on-line reservoir/pipette system, and average values of 1.00626 ±0.00222 and 1.00746 ±0.00159 per atomic mass unit were determined for the first and second runs, respectively, which were separated by about one month. Argon isotope abundances, corrected for blank, discrimination, and radioactive decay, are given in Supplementary Table 1. Ages for each step were calculated using interference corrections summarized by Renne et al. (2005b), the decay constants of Steiger and Jäger (1977), and with a J-value of (1.391 ±0.008) x 10^{-4} determined from the standard. The plateau age for each analysis is the inverse variance weighted mean of all steps. All uncertainties regarding $^{40}Ar/^{39}Ar$ data and ages herein are given at the 68% confidence level, and do not include systematic errors from decay constants or the age of the standard.

References in for this supplementary information:

Nomade, S., Renne, P.R., Vogel, N., Deino, A.L., Sharp, W.D., Becker, T.A., Jaouni, A.R., and Mundil, R., 2005, Alder Creek sanidine (ACs-2): A Quaternary Ar-40/Ar-39 dating standard tied to the Cobb Mountain geomagnetic event: Chemical Geology, v. 218, p. 315-338.

Renne, P.R., Mundil, R., Min, K., and Ludwig, K.R., 2005, Intercalibration of the U-Pb and Ar-40/Ar-39 geochronometers: Status, prognosis, and proscription: Geochimica et Cosmochimica Acta, v. 69, p. A321-A321.

Steiger, R.H., and and Jäger, E., 1977, Subcommission on geochronology: convention on the use of decay constants in geo- and cosmochronology: Earth Planet. Sci. Lett., v. 36, p. 359–362.

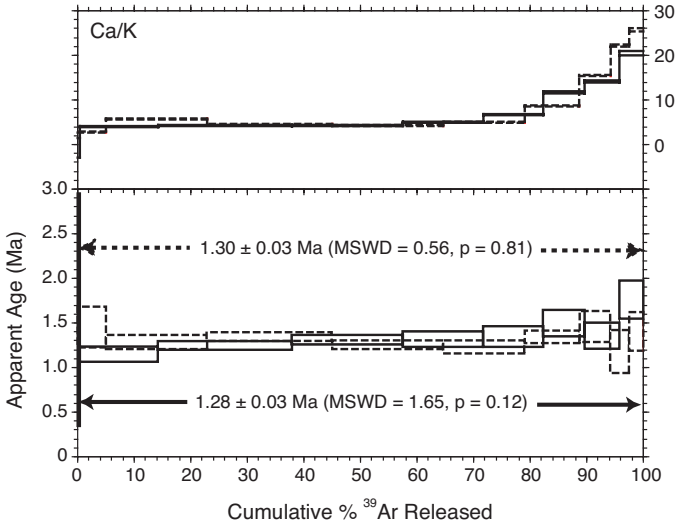

Supplemental Figure 1. Apparent $^{40}Ar/^{39}Ar$ age and Ca/K spectra for subsamples of basalt from Cerro Toluquilla volcano.

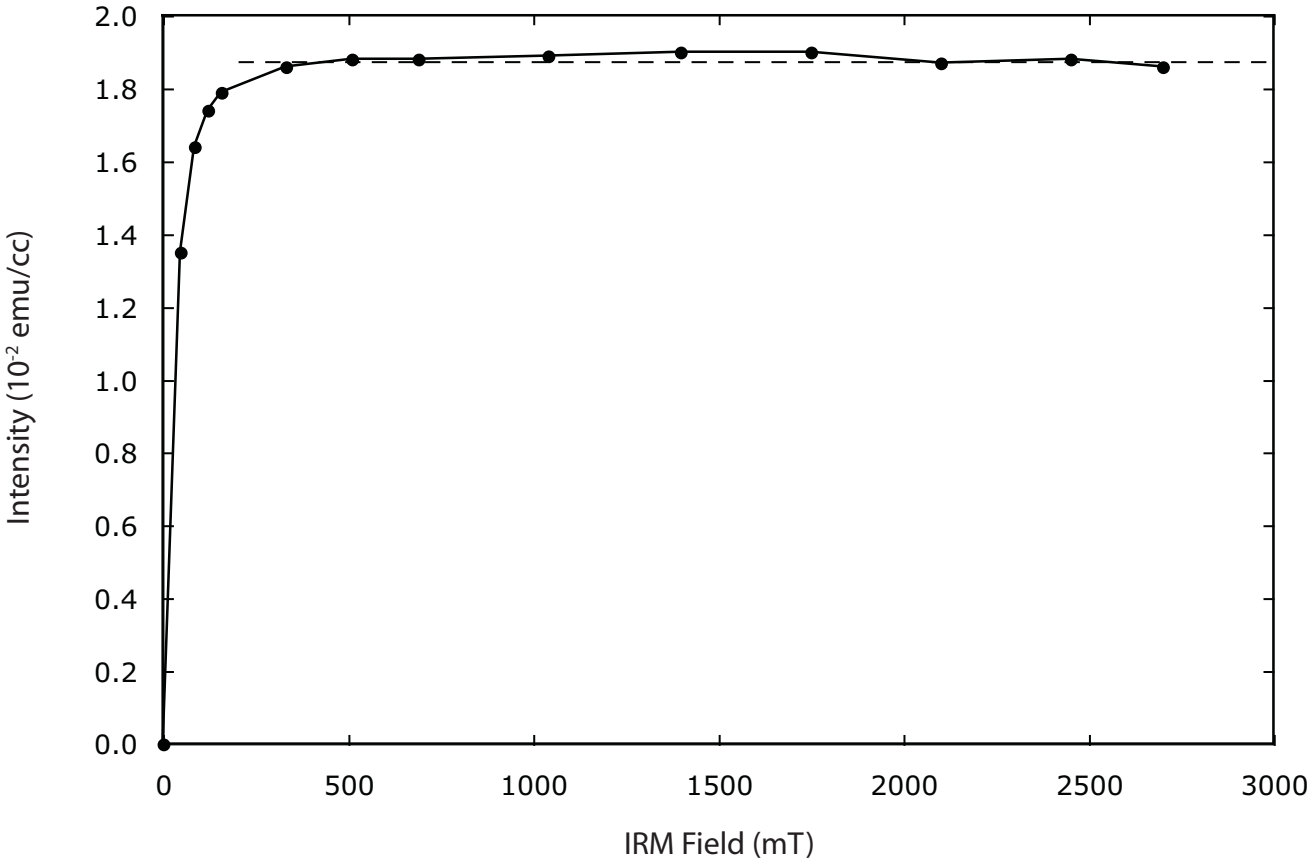

Supplemental Data - Figure 2. Typical isothermal remanent magnetization (IRM) acquisition curve for an individual lapillus. The plateau in intensity after ~300 mT indicates that the primary magnetic mineral phase is a cubic spinel. There is no indication of hematite.

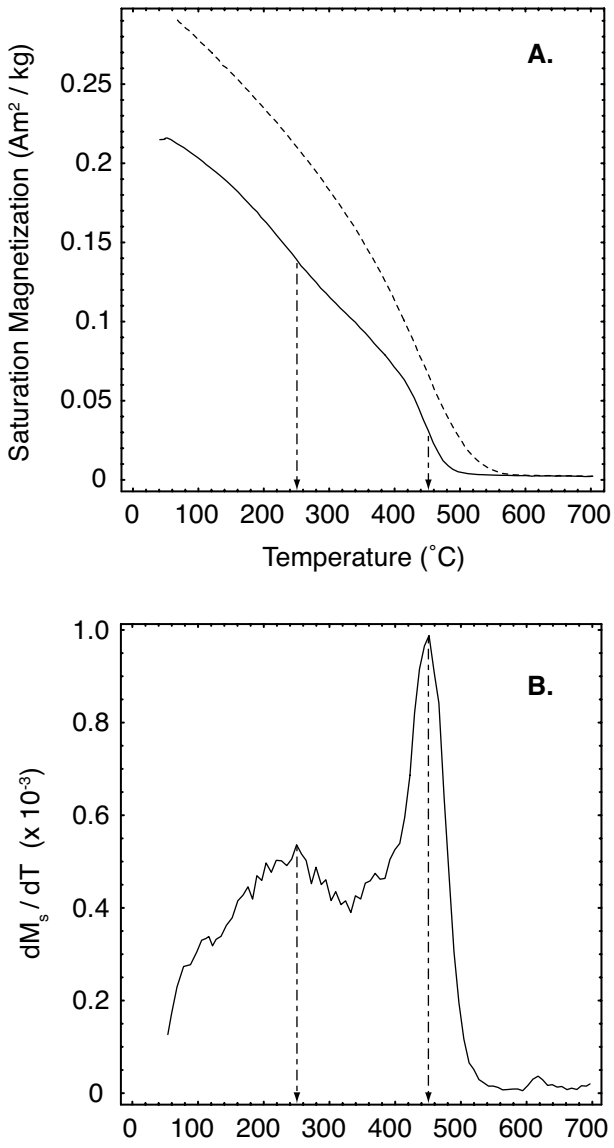

Supplemental Data - Figure 3. (A) Strong-field thermomagnetic curve measured using a 655 mT field for a single lapillus from the Xalnene tuff. Heating (cooling) curve is shown in solid (dashed) lines. (B) Smoothed first derivative of the heating cycle with dashed arrows indicating the temperatures where M_s changes most dramatically. The change occurring at ~250˚C is associated with traces of hydrous alteration products that could not be removed from the lapillus prior to measurement. The peak at 450˚C is corresponds to an unoxidized titanomagnetite of composition $Fe_{2.76}Ti_{0.24}O_4$ (Lattard et al., 2006).

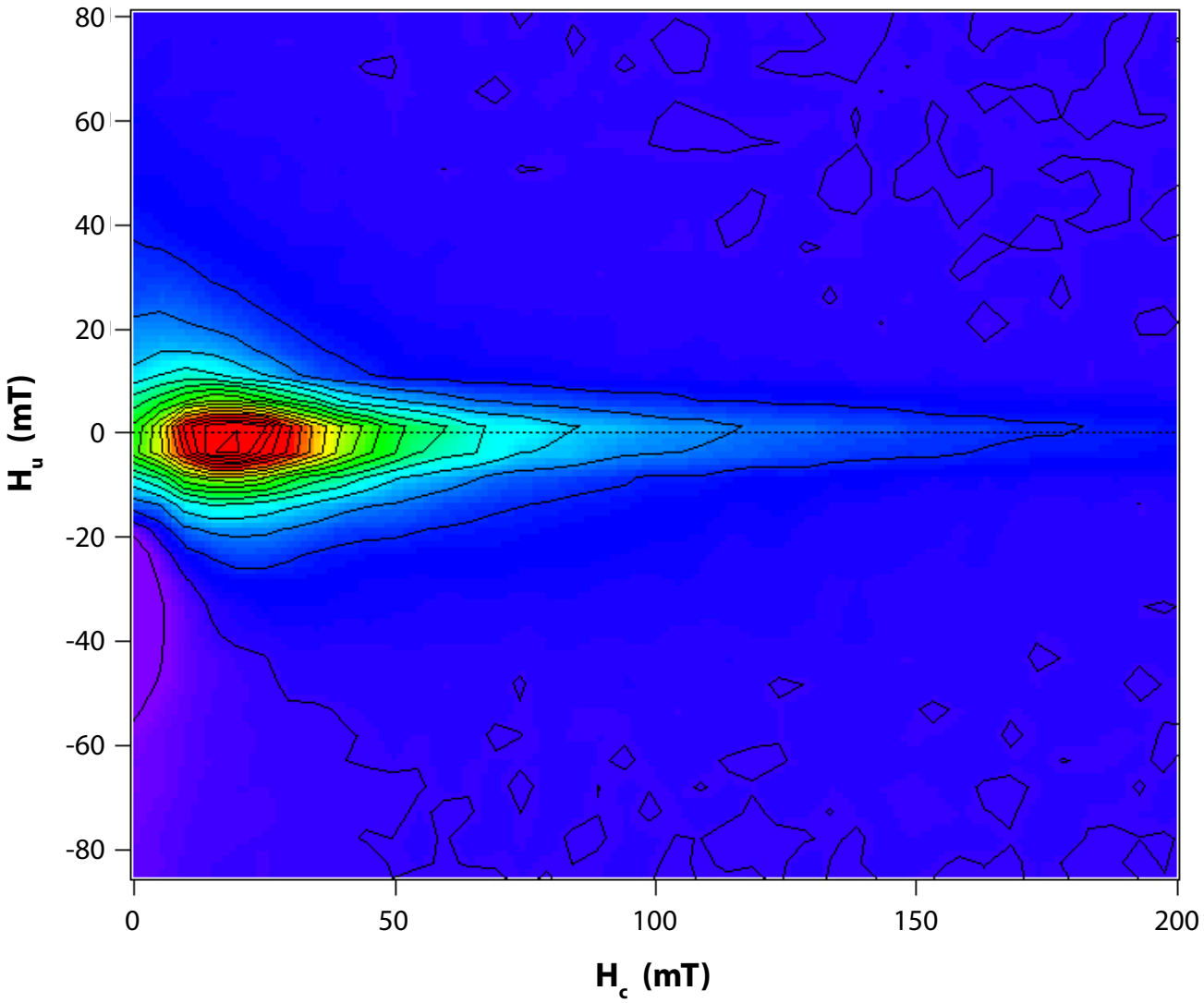

Supplemental Data - Figure 4. Typical first-order reversal curve (FORC) diagram for an individual lapillus. The diagram shows a single population of largely non-interacting single domain grains with a modal coercivity of 20 mT. A fraction of the titanomagnetite grains in the lapillus have coercivities as high as 150 mT.

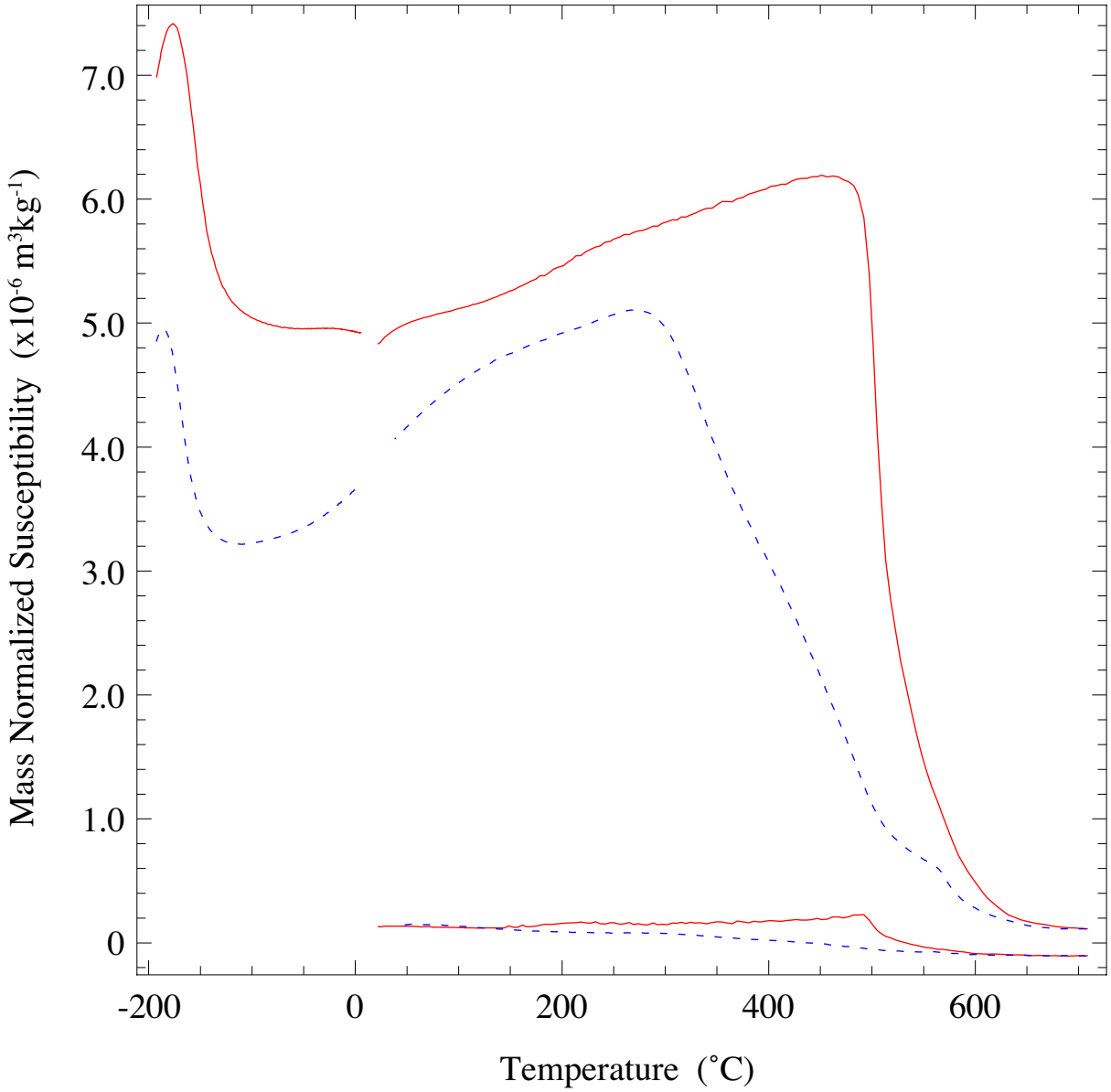

Supplemental Data - Figure 5. Mass normalized susceptibility as a function of temperature for a crushed sample of lava from Cerro Toluquilla. The red (blue) curves signify the heating (cooling) cycle of the experiment, which was run using an applied field of 200 Am^{-1} at 976 Hz. The lower pair of curves with maximum values no larger than 0.5 x 10^{-6} m^3kg^{-1} are the out-of-phase component of susceptibility. The Curie temperature of the sample is 503˚C, as determined using the differential technique on the in-phase heating curve, which corresponds to a titanomagnetite of composition $Fe_{2.83}Ti_{0.17}O_4$ (Lattard et al., 2006). The peak near -175˚C corresponds to the Curie temperature of titanoilmenite with composition ~$Fe_{1.04}Ti_{0.96}O_3$ (Dunlop and Özdemir, 1997). This dual phase mineral assemblage is further supported by thin section observations showing fine intergrowths of magnetite and ilmenite.

Power (W)	^{40}Ar (nA)	±s (nA)	^{39}Ar (nA)	±s (nA)	^{38}Ar (nA)	±s (nA)	^{37}Ar (nA)	±s (nA)	^{36}Ar (nA)
34530-01 D=1.00626 ±0.00222									
3	0.175260	0.000283	0.003488	0.000046	0.000134	0.000007	0.004783	0.000093	0.000525
6	0.271843	0.000532	0.012430	0.000061	0.000297	0.000008	0.035584	0.000171	0.000706
9	0.207165	0.000363	0.015239	0.000063	0.000248	0.000008	0.035597	0.000290	0.000426
12	0.176035	0.000335	0.013488	0.000065	0.000234	0.000007	0.029568	0.000162	0.000368
15	0.170271	0.000318	0.010006	0.000064	0.000190	0.000007	0.025919	0.000134	0.000411
18	0.159353	0.000484	0.006579	0.000032	0.000186	0.000007	0.028965	0.000181	0.000420
21	0.125941	0.000390	0.003882	0.000039	0.000115	0.000007	0.030423	0.000227	0.000350
25	0.085145	0.000227	0.002295	0.000027	0.000086	0.000005	0.025901	0.000169	0.000252
30	0.076083	0.000180	0.001645	0.000023	0.000073	0.000006	0.021420	0.000144	0.000226
34530-02 D=1.00746 ±0.00159									
2	0.043327	0.000471	0.000723	0.000066	0.000039	0.000009	-0.000331	0.000804	0.000131
5	0.530714	0.000680	0.019168	0.000152	0.000516	0.000014	0.038249	0.000905	0.001501
8	0.685148	0.002246	0.033051	0.000112	0.000711	0.000014	0.071728	0.000866	0.001766
11	0.741149	0.001376	0.027175	0.000097	0.000716	0.000014	0.057861	0.000848	0.002031
14	0.766728	0.001189	0.019993	0.000180	0.000701	0.000015	0.048900	0.000898	0.002241
17	0.807703	0.001097	0.014662	0.000152	0.000664	0.000015	0.049694	0.000911	0.002467
20	0.638576	0.000997	0.010093	0.000091	0.000500	0.000013	0.059742	0.000882	0.001957
24	0.485398	0.000909	0.008656	0.000072	0.000376	0.000012	0.061733	0.000894	0.001486
30	0.377510	0.000742	0.005752	0.000087	0.000305	0.000012	0.059772	0.000972	0.001141

±s (nA)	%^{40}Ar*	Age (Ma)	±s (Ma)
0.000010	11.4	1.440	0.232
0.000011	23.3	1.278	0.079
0.000008	39.3	1.339	0.047
0.000009	38.2	1.250	0.053
0.000009	28.7	1.225	0.073
0.000005	22.0	1.339	0.076
0.000009	17.8	1.452	0.180
0.000007	12.6	1.176	0.245
0.000004	12.1	1.399	0.217
0.000013	10.9	1.642	1.301
0.000019	16.4	1.141	0.085
0.000015	23.8	1.240	0.046
0.000015	19.0	1.302	0.057
0.000016	13.6	1.313	0.082
0.000016	9.7	1.344	0.116
0.000015	9.4	1.496	0.145
0.000014	9.6	1.345	0.149
0.000014	10.7	1.757	0.212

Supplemental Data - Table 2. Paleomagnetic Results for Valsequillo Reservoir Area Samples

Sample	Demagnetization Style	Range	Dec. (˚)	Inc. (˚)	a_{95} (˚)	n	Polarity
Toluquilla Lava - Characteristic Remanence Magnetization (ChRM)							
TOL07.01	AF	80-120 mT	181.6	-32.5	0.9	3	R
TOL07.02	AF	70-120 mT	173.1	-24.1	1.9	4	R
TOL07.03	AF	25-120 mT	175.1	-33.7	0.8	10	R
TOL07.04	AF	25-120 mT	171.8	-29.1	1	10	R
TOL07.05	AF	35-120 mT	171.3	-31.5	2.1	10	R
TOL07.06	Thermal	450-580˚C	174.5	-27.6	4.7	7	R
TOL07.07	Thermal	50-350˚C	169.5	-51.3	2.9	5	R
TOL07.08	Thermal	500-580˚C	174.6	-33.5	5.2	5	R
TOL07.09	Thermal	525-600˚C	184.4	-28	3.4	4	R
TOL07.10	Thermal	525-600˚C	178	-29.8	2.4	5	R
TOL07.11	AF	30-100 mT	180.7	-35.3	1.9	9	R
TOL07.12	AF	30-120 mT	180	-40.3	4	9	R
Fisher Mean	Hybrid		176.3	-33.1	4.3	12	R
Toluquilla Lava - Secondary Magnetizations							
TOL07.01	AF	7-70 mT	66.8	11.9	0.5	13	N
TOL07.01	AF	NRM-5 mT	349.7	5.2	4.9	4	N
TOL07.02	AF	NRM-60 mT	29.2	-22.6	2.1	16	R
TOL07.03	AF	NRM-21 mT	354	-10	2.7	11	R
TOL07.04	AF	NRM-21 mT	351	-13.5	2.7	10	R
TOL07.05	AF	NRM-30 mT	0.2	-21.8	1.1	12	R
TOL07.06	Thermal	150-425˚C	39.3	-86.7	8	6	R
TOL07.06	Pre-AF	NRM-13 mT	353.1	-14.5	2.2	8	R
TOL07.07	Thermal	NRM-13 mT	351.8	-6.9	2.6	8	R
TOL07.08	Thermal	50-450˚C	9.1	-76.4	9.6	8	R

TOL07.08	Pre-AF	NRM-13 mT	352.8	-16.2	1.8	8	R
TOL07.09	Thermal	150-500˚C	8.8	-80.5	5.3	8	R
TOL07.09	Pre-AF	NRM-13 mT	354.8	-11.8	2.8	9	R
TOL07.10	Thermal	50-500˚C	39.7	-86.4	14.1	10	R
TOL07.10	Pre-AF	NRM-13 mT	355.7	-10	2.9	8	R
TOL07.11	AF	NRM-25 mT	357.2	-10.7	3.2	12	R
TOL07.12	AF	NRM-25 mT	357.1	-13.1	3.1	12	R
Group 1	Thermal		15.9	-82.7	6	4	R
Group 2	AF		354	-11.1	4.6	10	R